Environmental Science: Atmospheres

ROYAL SOCIETY OF CHEMISTRY

PAPER

View Article Online
View Journal | View Issue

Cite this: *Environ. Sci.: Atmos.*, 2025, **5**, 636

A pulsed laser photolysis – pulsed laser induced fluorescence study of the kinetics and mechanism of the reaction of HgBr with NO_2 and O_2†

Dieter Bauer,[a] Deanna Donohoue[ab] and Anthony Hynes *[a]

Received 13th November 2024
Accepted 30th March 2025

DOI: 10.1039/d4ea00148f

rsc.li/esatmospheres

The kinetics of the reactions of mercurous bromide (HgBr) with NO_2 and O_2 have been studied using the pulsed laser photolysis – pulsed laser induced fluorescence technique in nitrogen, air and helium at room temperature and as a function of pressure. For reaction with NO_2, temporal profiles showed good pseudo-first order behavior and we see a three-body recombination and obtain rate coefficients of ~1–7 × 10^{-11} cm^3 per molecules per s over the pressure range 50–700 Torr in nitrogen. As expected, He is a less efficient 3rd body and rates are somewhat slower. We monitored the presence of a reduction channel regenerating Hg(0) and saw no evidence for it occurring. We obtained temporal profiles of HgBr at pressures of up to 500 Torr of O_2 demonstrating that laser induced fluorescence has adequate sensitivity as a concentration diagnostic in laboratory studies. The temporal profiles showed no evidence for any reaction between HgBr and O_2 at room temperature.

Environmental significance

Mercury is a potent neurotoxin and global pollutant. Concerns about its impact on the environment have led to 128 countries signing the Minamata Convention on Mercury, a legally binding international treaty, with the goal of reducing anthropogenic emissions of Hg. In the atmosphere mercury exists primary as gas phase elemental mercury, Hg(0). To be efficiently deposited and incorporated into terrestrial ecosystems Hg(0) must undergo atmospheric oxidation to stable mercuric compounds and multiple models have been developed to predict mercury cycling. However, the elementary reactions and the rate coefficients that are used in these models are based on computational chemistry and there is very little experimental data to support the calculated rates and reaction mechanisms. In this work we present results on a laboratory study of the kinetics and mechanism of the reaction of HgBr with NO_2, one potential route to a stable mercuric reaction product.

Introduction

A detailed understanding of the biogeochemical cycling of mercury and the routes to the production of organomercury compounds in terrestrial ecosystems is a critical issue from a human health perspective. Direct exposure to mercury is primarily through the ingestion of methylmercury from fish consumption.[1] Wet or dry deposition of oxidized mercury is an important step in a complex process that involves both chemistry and microbiology and eventually produces alkyl mercuric compounds. Consequently, an understanding of the overall budget and mechanisms of chemical transformation of mercury in both its elemental and combined forms is critically important. Hg(0) is almost insoluble in water, has a low deposition rate, and estimates of its atmospheric lifetime are variable ranging from a few months to more than one year.[2,3] The typical background concentrations of Hg(0) in unpolluted environments range from 1.2–2 ng m^{-3} in the northern hemisphere and 1–1.5 ng m^{-3} in the southern hemisphere where 1 ng m^{-3} is ~3 × 10^6 atoms per cm^3 or ~120 ppq (parts per quadrillion). Concentrations in both hemispheres have decreased over the past two decades.[4] Observations of Hg(0) concentrations in polar regions have demonstrated that Hg(0) undergoes rapid chemical reaction in the polar spring, and it is now generally accepted that the initial step in the Hg(0) oxidation process, in the polar atmosphere and globally, is the three body recombination of Hg(0) with Br atoms to give mercurous bromide, HgBr.[5]

However, HgBr is unstable and will dissociate to reactants unless it undergoes further reaction to form a stable mercuric compound. Over the past decade multiple models of the atmospheric oxidation process have been developed to explain the global distribution of Hg(0) concentrations, and deposition measurements of oxidized mercury. Nevertheless, the experimental database on the rate coefficients and mechanisms of potentially important atmospheric reactions is very limited or nonexistent in which case models rely on *ab initio* calculations. *Ab initio* calculations are challenging because of the necessity to

[a]*Department of Atmospheric Sciences, Rosenstiel School of Marine, Atmospheric and Earth Science, 4600 Rickenbacker Causeway, Miami, FL 33149, USA. E-mail: ahynes@miami.edu*

[b]*Department of Chemistry, Lawrence University, 711 East Boldt Way, Appleton, WI 54911, USA*

† Electronic supplementary information (ESI) available. See DOI: https://doi.org/10.1039/d4ea00148f

account for the relativistic effects associated with the heavy mercury atom. Dibble and coworkers have reported calculations and experimental measurements concluding that HgBr can react rapidly with both NO_2 and HO_2.[6,7] Based on this work, Horowitz *et al.*[8] concluded that the Hg(0) + Br recombination followed by reaction of HgBr with NO_2 and HO_2 is the primary oxidation mechanism for Hg(0) on a global scale.

$$HgBr + NO_2 \rightarrow \text{product} \quad (R1)$$

$$HgBr + NO_2 \rightarrow BrHgNO_2 \quad (R1a)$$

$$HgBr + NO_2 \rightarrow Hg + BrNO_2 \quad (R1b)$$

A more recent work suggests reaction with O_3 may be more important.[9] In this work we report measurements of the rate coefficients and mechanism of the reaction of HgBr with NO_2 and O_2 and compare this with recently published measurements from Dibble and coworkers.[6,10] Although we see no evidence for reaction with O_2 at room temperature we demonstrate that laser induced fluorescence has adequate sensitivity to monitor HgBr in laboratory studies at high O_2 concentrations.

Experimental section

The experimental approach utilized the pulsed laser photolysis – pulsed laser induced fluorescence technique and is similar to multiple other studies published from this laboratory.[11] The 4th harmonic of a Nd-YAG laser is used to photolyze a suitable precursor generating a low concentration of the free radical of interest, which is then monitored using laser induced fluorescence with a frequency doubled Nd-YAG pumped dye laser. The lasers operate at a repetition frequency of 10 Hz and the time delay between the lasers is varied to obtain a temporal profile of the free radical. Most of our previous work has focused on kinetic studies of the OH radical, but the basic approach in this work was very similar. A schematic of the experimental setup is shown in Fig. 1. The free radical of interest, HgBr, was produced by photolysis of $HgBr_2$ using the fourth harmonic of a Nd-YAG laser at 266 nm.

$$HgBr_2 + h\nu_{266\ nm} \rightarrow HgBr + Br \quad (R2)$$

The HgBr radical was monitored using an approach described by Donohoue,[12] exciting the $D^2\Pi_{3/2}$–$X^2\Sigma$ (2–0) transition at ~256 nm. The $D^2\Pi_{3/2}$ (2) vibrational level undergoes collision induced transfer to the $B^2\Sigma$ state and the fluorescence from the $B^2\Sigma$–$X^2\Sigma$ transition in the visible wavelength region is observed at 485–505 nm.[13] The fluorescence is primarily characterized by transitions from a highly excited $B^2\Sigma$ state to the ground state of the $X^2\Sigma$ level. The maximum fluorescence was observed at ~502 nm, mainly the (22,0) transition. However, the observed peak contains fluorescence from all transitions, which have a $\Delta v = 22$ such as (22,0), (23,1), and (24,2). Resolved fluorescence measurements[12] indicate that the intensity of the B–X band increases by a factor of three relative to the D–X band as pressure is increased from 80 to 400 tour in N_2 but we are not aware of any

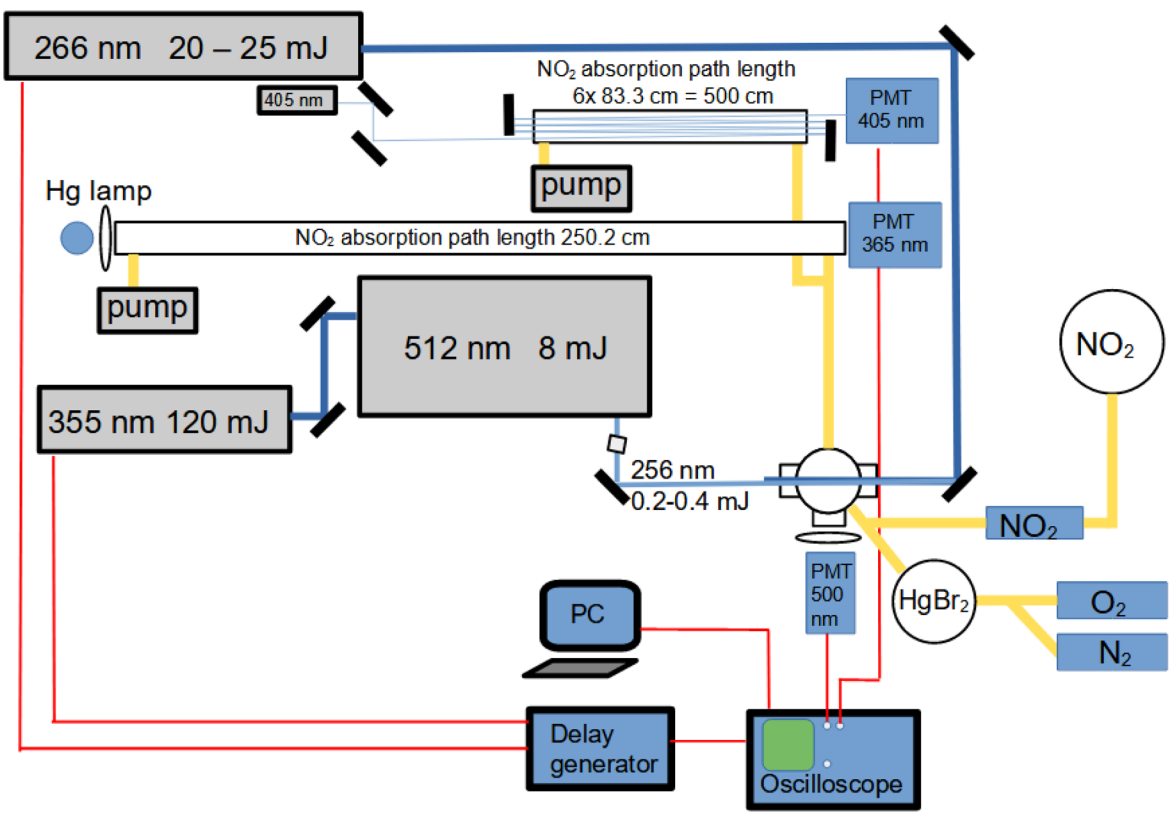

Fig. 1 Schematic of the experimental setup.

quantitative measurements of the rate of collision induced crossing between the D and B states. The $B^2\Sigma$–$X^2\Sigma$ fluorescence was monitored with a photomultiplier tube (PMT) using a filter pack consisting of a 500 ± 8 nm interference filter and a long pass filter. Hg(0) was detected by exciting the 6^3P_1–6^1S_0 transition at 253.7 nm and by monitoring the resonance fluorescence with a PMT equipped with a 254 nm interference filter. The photomultiplier outputs were amplified, and fed to a 200 MHz digital oscilloscope to obtain the integrated voltage for, typically, 64 laser shots. The temporal profile of the HgBr was obtained by varying the delay between the photolysis and probe lasers using a digital delay generator. The whole experimental sequence was controlled by a computer using a program written in python which set and controlled the delay sequence and read the integrated PMT voltage at each delay setting. The experimental procedure involved scanning from short to long delay times, and then returning to a normalization delay. The sequence was repeated twice with different delay times, again returning to the normalization delay after each delay scan. The probe laser was then blocked and scattered light from the photolysis laser was monitored as a function of delay time. The sets of delay scans were then normalized to give a complete concentration time profile and, finally, the photolysis scatter was subtracted from the normalized concentration time profile. The photolysis scatter was less than 5% of the maximum signal an was only measurable for 20 μs. Experiments were performed in a Pyrex reaction vessel at the temperature in the laboratory which was 22 °C. The reaction vessel was 8 cm in length and 2.5 cm in diameter. Four side arms were attached to the center. The photolysis and probe laser beams counter propagated through two of the side arms and fluorescence was detected perpendicular to the laser beams through a third side arm. The experiments were carried out under slow flow conditions with flows along the long axis of the cell ranging from 1 to 5 standard liters per minute (SLPM). This corresponded to linear flow rates between 15 and 70 cm s^{-1}. Gas flow rates were measured using calibrated mass flow controllers and mass flow meters. Pressures were measured using capacitance manometers. $HgBr_2$ was introduced into the reactant mixture by flowing the premixed gases through a Pyrex tube containing a porcelain boat filled with solid $HgBr_2$ powder. This tube was located immediately before the reaction vessel and was not heated. We estimated that we obtained an $HgBr_2$ concentration of $\sim 4 \times 10^{11}$ molecules per cm^3 in the gas mixture which was determined by pyrolysis and measurement of [Hg(0)] as discussed below. This is about an order of magnitude lower than calculated equilibrium vapor pressures (4.3×10^{12}, 303 K (ref. 6)) and (2×10^{14}, 338 K (ref. 9)).

The gas mixture then passed through an absorption cell, cold trap and pump. The different length and design of the absorption cells is discussed below.

In situ measurements of stable reactants

In this experimental approach the accuracy of the rate coefficient is dependent on the accuracy with which the concentration of the reactants in pseudo first order excess can be determined. In our experience the most accurate determination is obtained by monitoring the excess reactant *in situ* using absorption spectroscopy. Clearly this requires a suitable absorption feature with an adequate absorption cross section. In prior work on the kinetics of the reaction of OH with NO_2, we monitored the NO_2 concentration using absorption cells located before and after the reaction vessel, using absorption of the 365 nm line of a Hg lamp and absorption of the output of a Deuterium lamp between 200 and 380 nm using a monochromator and an optical multichannel analyzer.[11] In our prior work the absorption cell lengths were limited to 100 cm and we obtained excellent agreement between concentrations using the atomic line, broadband absorption and flow calculations. To extend the range of concentrations that can be monitored *in situ* we used 2 different absorption cells with lengths of 0.83 and 2.5 m. This allowed us to measure very low concentrations of NO_2, and it also allows us to measure low concentrations of Hg(0) and provide an absolute calibration of our Hg(0) LIF signal. NO_2 was purified by freeze–pump cycles at 77 K and mixtures containing approximately 3% NO_2 in nitrogen or helium were prepared manometrically in 20 L Pyrex bulbs. An accurate bulb concentration was then measured using the absorption of the 365 nm mercury line which has a well established[11,14] cross-section of $(5.75 \pm 0.17) \times 10^{-19}$ cm^2. We wanted to have the option to use a 405 nm diode laser for absorption measurements, so a second absorption cell was placed in series with the 365 nm cell and the absorption cross-section at 405 nm was determined relative to the 365 nm absorption cross-section. We obtained an absorption cross section of 4.8×10^{-19} cm^2. Both the 365 nm mercury line and the 405 nm diode laser line were then used for *in situ* measurements of the NO_2 concentration during experiments. Initial experiments at lower NO_2 were performed using the 405 nm diode laser which was multi passed through an 83 cm absorption cell with typically six passes giving an absorption path length of 5 m. A beam splitter directed a small fraction of the 405 nm beam onto a photomultiplier tube to monitor the variability in diode laser output. After passage through the cell the transmitted beam was also monitored using a second photomultiplier tube. Output currents were measured with a picoameter and an oscilloscope and fed to a computer with measurements being recorded at 1 Hz. A similar approach was used for the 365 nm measurements.

Results and discussion

$HgBr_2$, HgBr, and Hg(0) background concentration measurements

We have measured the concentration of the $HgBr_2$ precursor using pyrolytic conversion of $HgBr_2$ to Hg(0). In this approach, developed by Landis *et al.*,[15] the gas mixture is flown over a KCl coated annular denuder which is heated to 500 °C in a tube furnace. We used an annular denuder which is identical to that described by Landis *et al.* Fig. 2 shows a measurement of the Hg(0) concentration profile in the 2.5 m absorption cell as a function of time using absorption of the 253.7 nm mercury line. After an initial flow of pure N_2 through the absorption cell

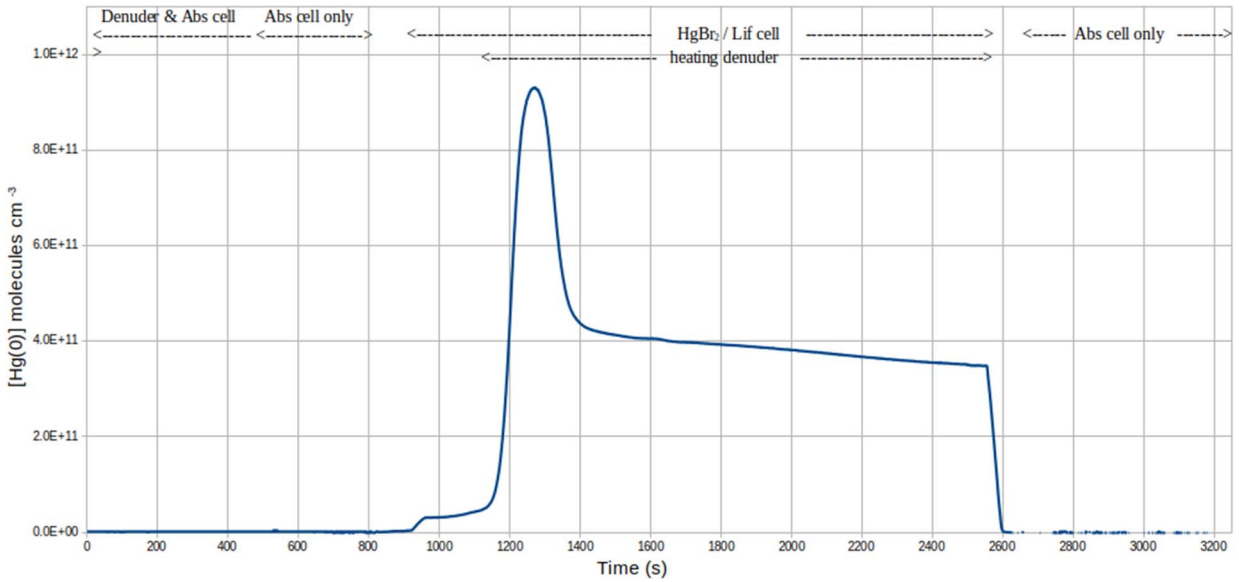

Fig. 2 Hg(0) temporal profile during pyrolysis of $HgBr_2$.

to establish an I_0, the $HgBr_2$ source and absorption cell are connected in line at 900 s. We see an increase in Hg(0) which corresponds to a background level of $\sim 3 \times 10^{10}$ atoms per cm^3 and this value was used to calibrate the mercury concentrations in Fig. 6 and 7. We speculate that this background Hg(0) comes from the dissociation of $HgBr_2$. At approximately 1100 s the denuder is heated to 500 °C and we see a spike in Hg(0) as the accumulated $HgBr_2$ decomposes eventually giving a close to steady state concentration of $\sim 4 \times 10^{11}$ atoms per cm^3 which corresponds to the $HgBr_2$ concentration at a flow of 5 SLPM. The typical 266 nm photolysis energy in the reaction volume is 15–20 mJ with a diameter of 0.5 cm. There is considerable uncertainty in the absorption cross section of $HgBr_2$ at 266 nm based on the literature measurements which were made at elevated temperatures.[16] We assume an absorption cross section of 1×10^{-18} cm^2 which gives a photodissociation efficiency of ~10% and an initial HgBr concentration of 4×10^{10} molecules per cm^3 assuming a quantum yield of 1.

$$HgBr + NO_2 \rightarrow \text{products} \quad (R1)$$

Experiments were carried out under pseudo first-order conditions. Typical NO_2 concentrations ranged between 1×10^{14} to 5×10^{15} molecules per cm^3, with an estimated HgBr concentration of $\sim 4 \times 10^{10}$ molecules per cm^3. There it's a significant uncertainty in this number but it's clear that the HgBr concentration is several orders of magnitude lower than the NO_2 concentration.

For reaction (R1) the HgBr temporal profiles were analyzed assuming simple pseudo-first order behavior to extract a pseudo-first order rate,

$$[HgBr]_t = [HgBr]_0 \exp(-k't) \quad (1)$$

where $k' = k[NO_2] + k_d$ where k is the bimolecular reaction rate and k_d is the background loss rate of HgBr by diffusion and any other background loss processes. HgBr decays were monitored over, typically, 4–5 1/*e* times (*i.e.* 1% of original signal). Decays were analyzed by fitting (eqn (1)) to the temporal profiles. Fig. 3a and b show several plots of ln[HgBr] *vs.* time at various NO_2 concentrations and a total pressure of 400 Torr in N_2 bath gas. These results are typical of data obtained in N_2 with a 2σ uncertainty of less than 2% and are tabulated in Table S1.† The plots show excellent linearity to at least 4 1/*e* times, *i.e.* 2% of the initial signal. In some cases we see slight deviations from linearity at very low signal levels which reflects uncertainties due to the normalization and background subtraction processes described above. Pseudo first order rates of up to $\sim 5 \times 10^5$ s^{-1} are measured. Measurement of such fast pseudo first order rates requires that scatter from the photolysis laser be minimized at very short delay times. We find that there are advantages to being able to measure such fast decays. Firstly, it enables us to see very fast equilibria that can occur in, for example, the reaction of OH with organic sulfides.[17,18] In addition, this allows us to use higher concentrations of the excess reactant and improves the precision of the rates extracted from pseudo first order plots. Fig. 4 shows a pseudo first order plot of the data points from Fig. 3a and b/Table S1.† The NO_2 concentrations are calculated from both flow and absorption measurements. The 2σ measure of precision of each point is plotted but is often smaller than the symbol size. The calculated rate coefficients and zero concentration offset together with the 2σ errors are tabulated for all the pseudo first order decay plots in Table S2.†

The pressure dependence of reaction (R1) was studied in nitrogen, helium and one measurement was made in air. Fig. 5 shows the pressure dependence of the rate coefficients obtained using NO_2 concentrations calculated from both absorption measurements and flow calculations. The rate coefficients are listed in Table S2 in the ESI.† There is typically good agreement

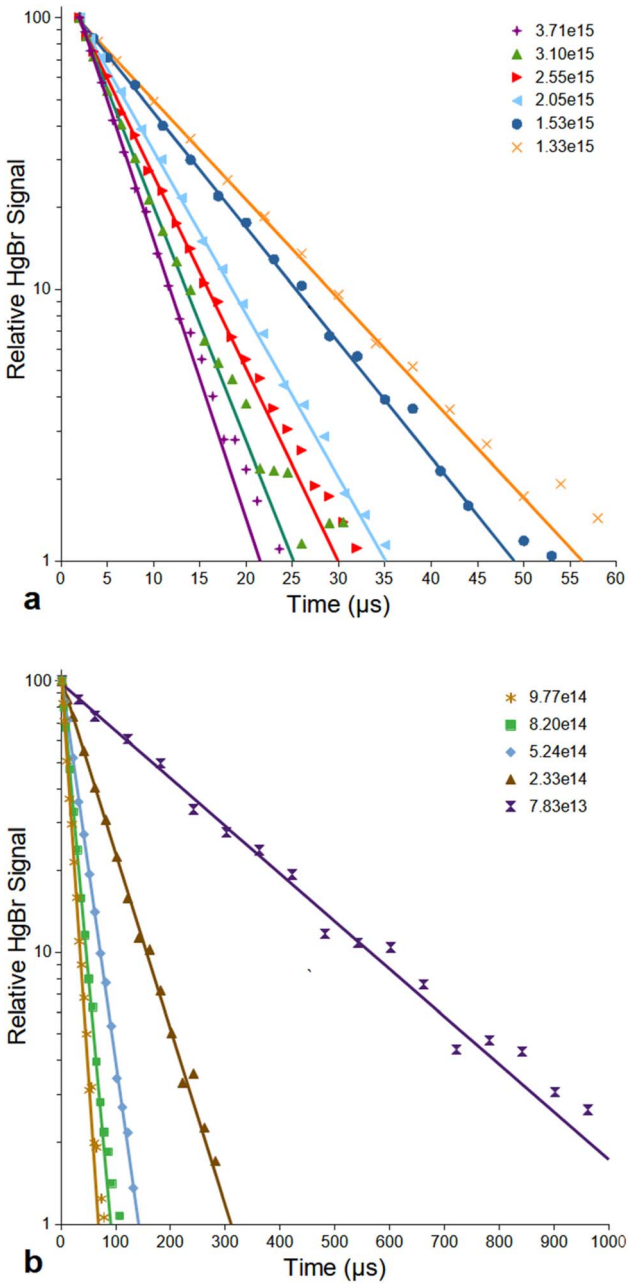

Fig. 3 (a) and (b) Temporal profiles of HgBr at several NO_2 concentrations at a total pressure of 400 Torr of N_2.

between the flow and absorption measurements, but the rates obtained using flows are systematically a few percent higher than those obtained from absorption. It is important to note that both sets of measurements ultimately depend on the use of an absorption measurement to calculate NO_2 concentration (*i.e.* in the initial 3% mixture in the 20 L Pyrex bulb and then directly *in situ*). We typically see larger zero offsets in the regression lines that used concentrations based on flows which is suggestive of a small systematic error in the flow calibrations at low flows. Consequently, we regard the rate coefficients based on concentrations determined by the *in situ* absorption measurements as being more reliable. There is a significant pressure dependence of the rate coefficient in both molecular nitrogen and helium. The single measurement in air is essentially identical to the measurement in nitrogen. As expected nitrogen shows a greater third body efficiency than helium although the scatter in the He data is larger than in the N_2 data, and, based on the single measurement in air, it appears that there is not a significant difference in the third body efficiency between oxygen and nitrogen.

Reaction (R1b). As we noted above, Jiao and Dibble[7] reported a computational study of reaction (R1) that suggested that a reduction channel operates in parallel with the oxidation channel and may be a significant fraction of the total reactive channel at low temperatures. The presence of a reduction channel (R1b) would be significant in assessing the atmospheric oxidation rate of Hg(0) since it would essentially constitute a null cycle in which Hg(0) is oxidized to Hg(I) in the addition reaction with Br but then partially reduced back to Hg(0) in the reaction of HgBr with NO_2. To assess the importance of a reduction channel we attempted to monitor the production of Hg(0) in reaction (R1b). Hg(0) was detected by exciting the 6^3P_1–6^1S_0 transition at 253.7 nm and by monitoring the resonance fluorescence with a PMT equipped with a 254 nm interference filter. First we needed to characterize the background level of Hg(0) in our system. We have a background level of Hg(0) equal to 3×10^{10} molecules per cm^3 in our experimental system which we attribute to the slow thermal dissociation of $HgBr_2$ in the flow system. As detailed above, we were able to measure this background concentration by absorption of the 253.7 nm line from a mercury lamp in the 2.5 m absorption cell and this allows us to obtain an absolute calibration of our Hg(0) LIF signal. In addition, as shown in Fig. 6 we have an additional background concentration of 4×10^{10} molecules per cm^3 generated by the photolysis laser which reaches a total steady state of the sum of these concentrations of approximately 7×10^{10} molecules per cm^3. The sum of the background Hg(0) plus the photolytically generated Hg(0) gives a steady state level of approximately 7×10^{10} molecules per cm^3. The Hg(0) LIF signal is observed after photolysis in the absence of a flow of $HgBr_2$ and or NO_2, as shown in Fig. 6. The figure shows the Hg(0) concentration profile measured by LIF at 253.7 nm as a function of laser pulse with a constant time delay between the photolysis and probe laser of 4 μs. The gas flow consists of N_2 with no flow of $HgBr_2$ or NO_2. For the first 110 laser pulses the photolysis laser is blocked. Prior to photolysis we see the steady state background [Hg(0)] of $\sim 3 \times 10^{10}$ molecules per cm^3 with absolute concentration obtained from absorption measurements. After the introduction of the photolysis beam, we see production of additional Hg(0) which continues for approximately 200 laser shots followed by the establishment of a steady state concentration. After the photolysis laser is blocked it takes approximately 200 laser shots to return to the steady state background concentration. We observed this behavior in both N_2 and He and the rise and decay times show a dependence on pressure and flow rate. We do not see this behavior in the rise time of HgBr which reaches its steady state concentration in a single photolysis shot. We speculate that this Hg(0) signal is produced by laser induced

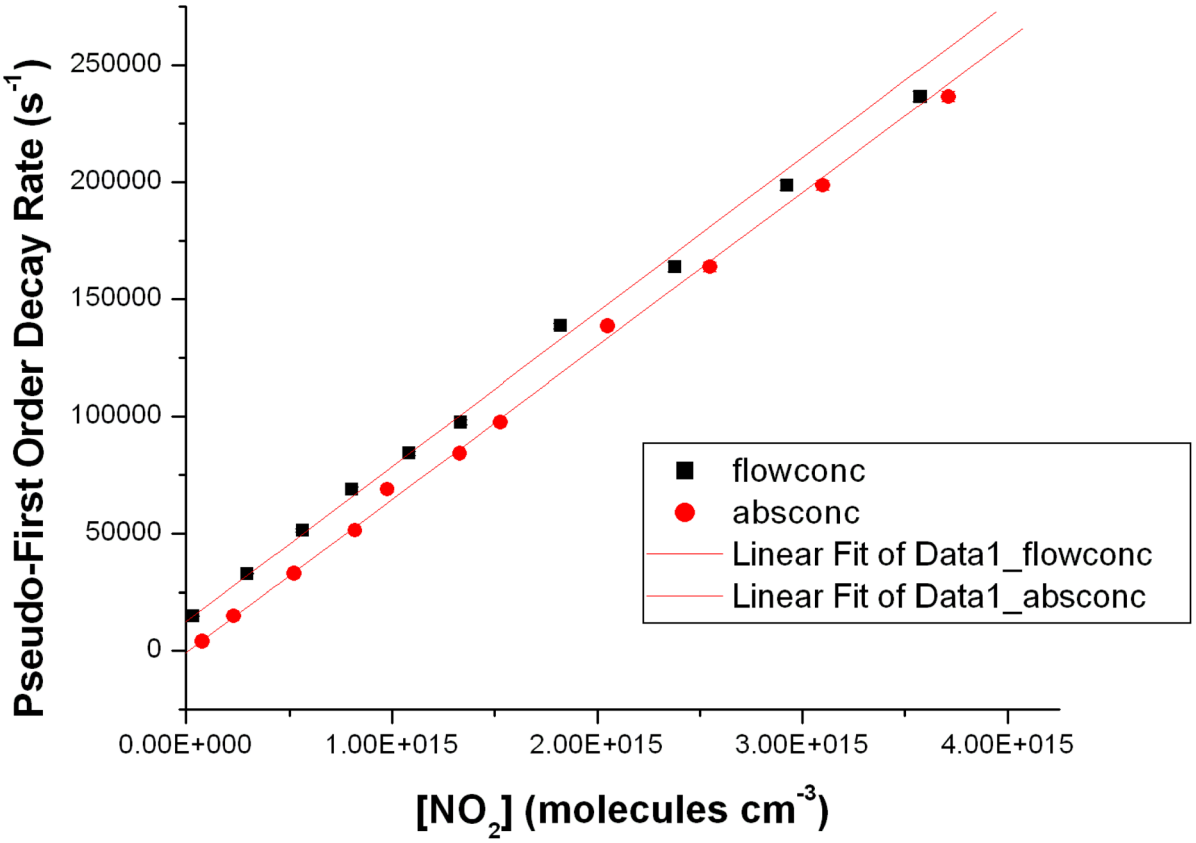

Fig. 4 Pseudo-first order decay rates as a function of NO_2 concentration for all 400 Torr data. The plot shows rates at NO_2 concentrations calculated using both flow (flowconc) and *in situ* absorption (absconc) measurements.

desorption of Hg(0) from the windows and walls of the reaction vessel. The reaction vessel has an internal volume of approximately 0.25 L. At a typical flow rate of 4 L min^{-1} it takes approximately 4 seconds to flush the cell completely. In practice there are dead zones in the sidearms which will not be flushed efficiently. If our hypothesis is correct, the photolysis beam desorbs Hg(0) from the entrance and exit windows and some portion of this is entrained into the reaction zone and is then detected by the probe beam. As we move from "no photolysis" to introducing the photolysis beam we see the initial rise in Hg(0) until we reach a point at which production is balanced by the loss from the flow out of the reaction vessel. Further work is required to establish the source and, if possible, eliminate this photolytic production of Hg(0).

To look for the presence of a reduction channel we need to monitor Hg(0) formation after photolysis of an $HgBr_2/NO_2$ mixture. Fig. 7 shows the temporal profile of Hg(0) measured by LIF at 253.7 nm in 100 Torr of He in the presence of NO_2 at a concentration of 3×10^{15} molecules per cm^3. The profile is obtained by taking a pre-photolysis point and then several post photolysis points at different delays and then repeating the sequence. At this pressure we obtain a rate coefficient for reaction (R1) of $\sim 4 \times 10^{-11}$ cm^3 per molecules per s. Hence the reaction proceeds with a pseudo-first order rate of 120 000 s^{-1} and a $1/e$ time of $\sim$8 μs. The reaction has essentially proceeded to completion in 40 μs. If we use the background concentration of Hg(0) of $\sim 7 \times 10^{10}$ atoms per cm^3, we can calibrate the concentration axis of Fig. 7 and estimate the importance of the reduction channel (R1b) by monitoring Hg(0) production. The pre-photolysis signal is $(6.83 \pm 0.21) \times 10^{10}$ atoms per cm^3. The average of the post photolysis signal is $(7.05 \pm 0.16) \times 10^{10}$ atoms per cm^3. Statistically we see no increase in Hg(0) as a function of delay time after photolysis suggesting that channel (R1b) is not significant.

Reaction (R3). Wu *et al.*[10] have suggested, based on density functional calculations, that HgBr and O_2 form a relatively unstable adduct but that this adduct could be significant fraction of total [HgBr] at upper tropospheric temperatures.

$$HgBr + O_2 \rightleftharpoons HgBrOO \quad (R3)$$

To estimate the significance of any reaction between HgBr and O_2, we measured HgBr temporal profiles at several O_2 partial pressures in N_2/O_2 mixtures at a total pressure of 500 Torr. Fig. 8 show a series of temporal profiles of the HgBr LIF signal with the signal normalized so that the initial HgBr LIF signal is 100 arbitrary units in each decay. Fig. 8 shows the temporal profiles on logarithmic scale. The decays do not follow simple pseudo-first order kinetics. We see an initial rise in the [HgBr] followed by decays at a rate of $\sim$50 s^{-1} which show no dependence on O_2 concentration. The decays are dominated by diffusion of the HgBr from the reaction volume and reaction

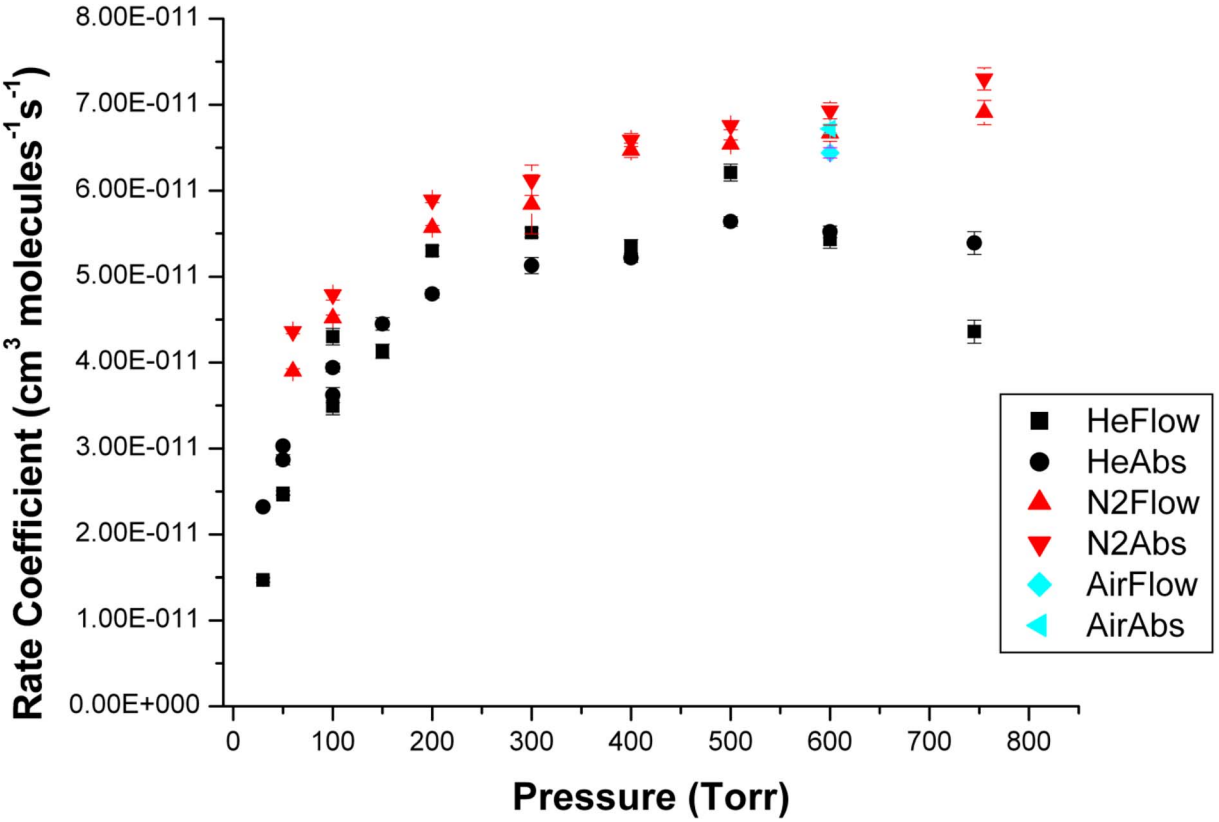

Fig. 5 Pressure dependence of the rate coefficients for reaction (R1) in N_2, air and He. Rates are shown for NO_2 concentrations calculated using both flow (*i.e.* HeFlow) and *in situ* absorption (*i.e.* HeAbs) measurements.

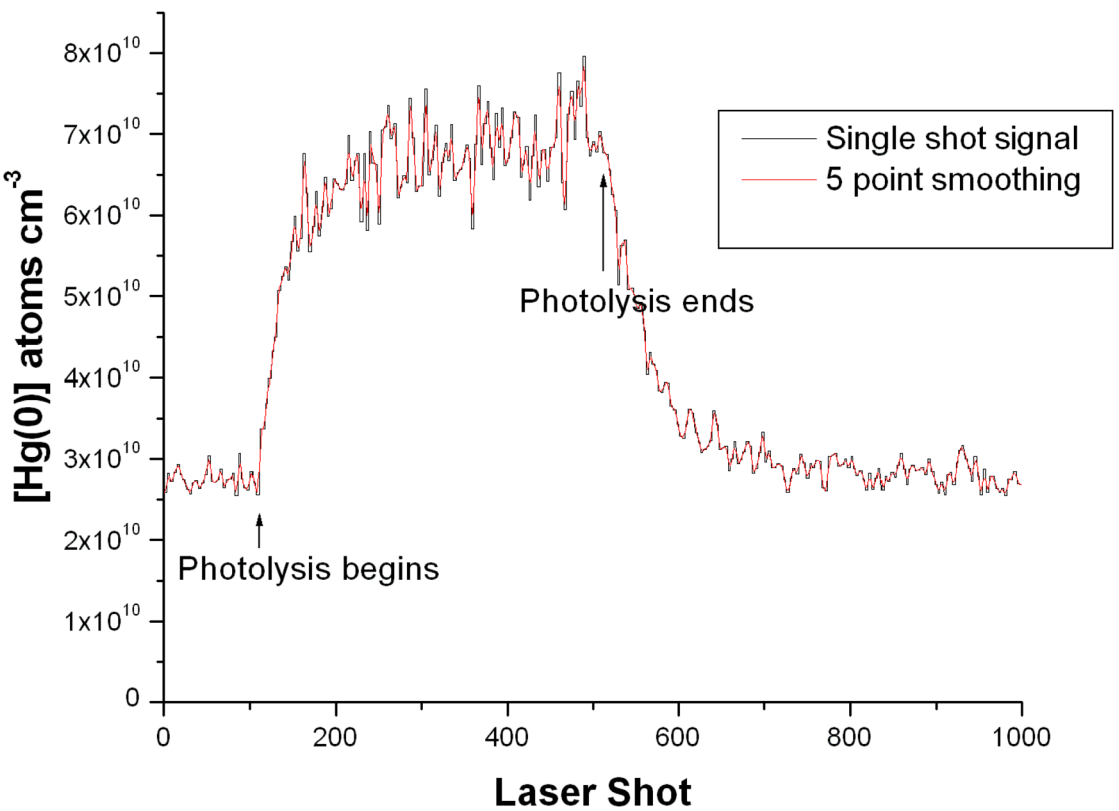

Fig. 6 Hg(0) concentration as a function of laser shots before and after the introduction of the photolysis laser.

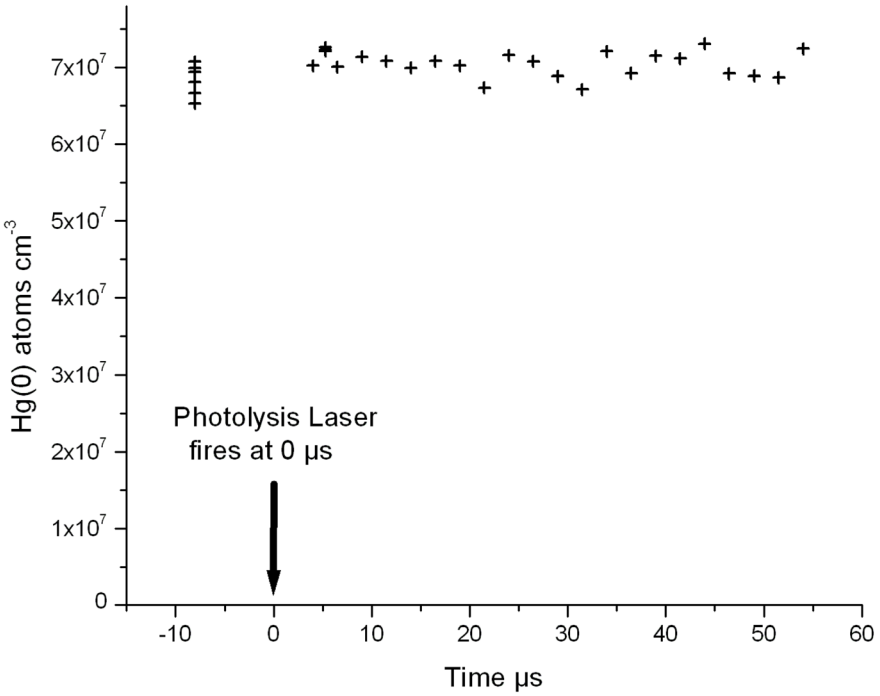

Fig. 7 Hg(0) as a function of delay time with an NO_2 concentration of 3×10^{15} molecules per cm^3 at a total pressure of 100 Torr in He.

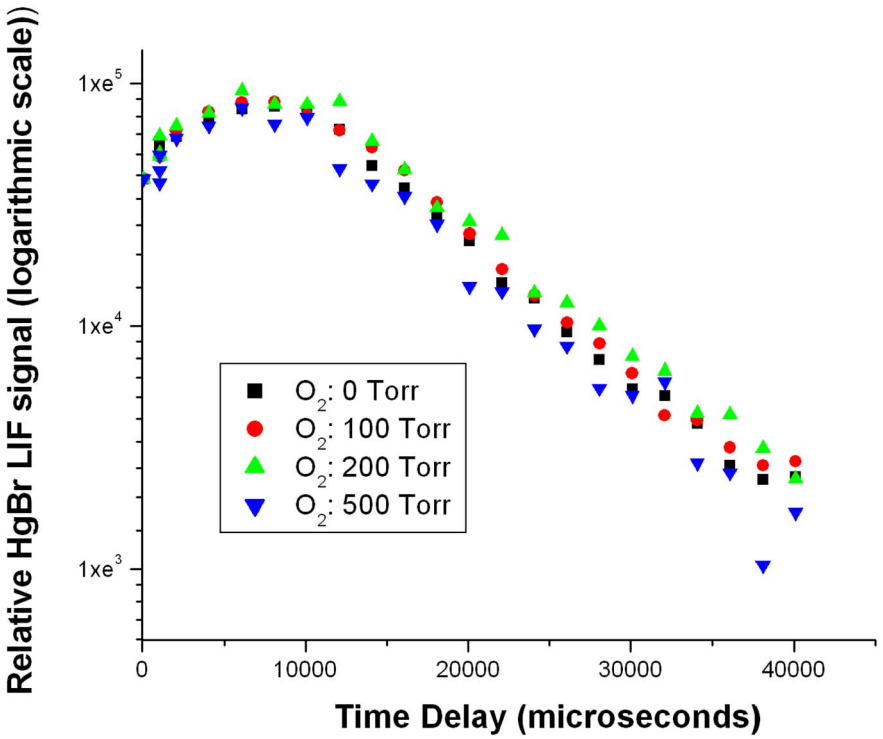

Fig. 8 Temporal profiles of HgBr in N_2/O_2 mixtures at a total pressure of 500 Torr at several partial pressures of O_2.

(R3) is too slow to be of any significance at room temperature. Lower temperature studies are required to determine the possible significance of the reaction at upper tropospheric temperatures. The initial rise in the HgBr concentration may be an indication of radiative cascading of vibrationally excited HgBr formed in the photolysis of $HgBr_2$. Fig. 9 shows a laser excitation spectrum of the HgBr product formed in the 213 nm photolysis of $HgBr_2$.[12] The HgBr product was monitored *via* the

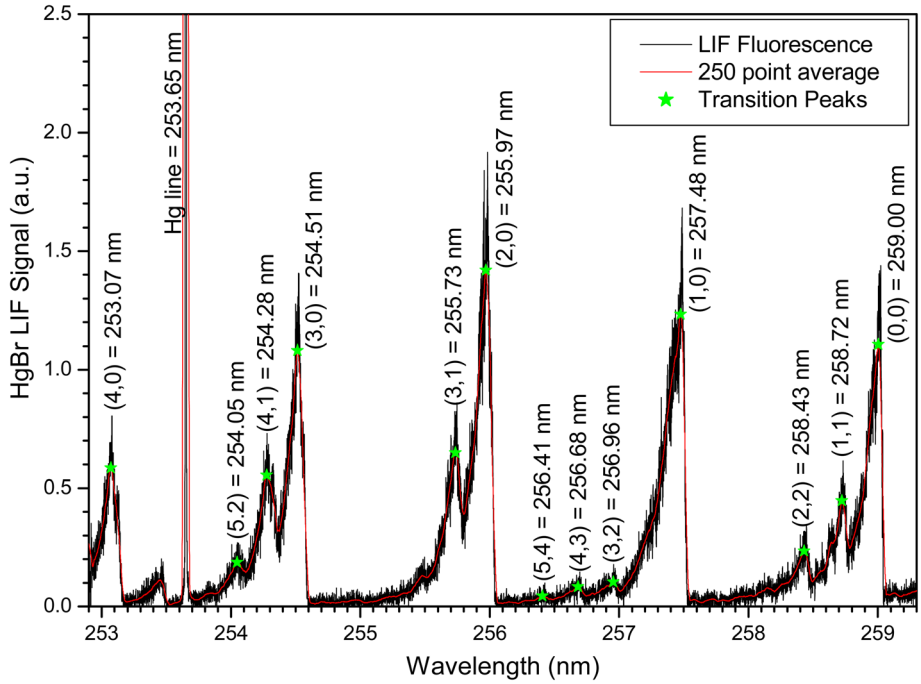

Fig. 9 Laser excitation spectrum of the HgBr product formed in the 213 nm photolysis of $HgBr_2$.[12]

$D^2\Pi_{3/2}$–$X^2\Sigma$ transition with fluorescence detection using a PMT with a 262 nm filter. The spectrum shows production of vibrationally excited HgBr with population of the $v = 1$–4 levels in the $X^2\Sigma$ ground electronic state. Both Wu *et al.*[6] and Gómez Martín *et al.*[9] published laser excitation spectra of HgBr with photolysis of $HgBr_2$ at 266 nm and HgBr detection using the $B^2\Sigma$–$X^2\Sigma$ transition. These excitation spectra also show transitions from vibrationally excited HgBr. None of these spectra were obtained under conditions that would likely show the nascent vibrational excitation of the HgBr product. This type of vibrational excitation can be problematic in kinetic studies if cascading of high vibrational levels to the ground vibrational state occurs on a time scale that is close to the removal of the ground state by reaction. Because of the very large rate coefficient for reaction (R1) we do not believe this is a potential artifact in these studies.

Comparison with previous work

In this work we use a similar approach to that recently published by Wu *et al.*[6] although there are some differences that we believe are significant. A comparison of our results in N_2 with those of Wu *et al.* are shown in Fig. 10. The slight difference in temperature, 313 K for Wu *et al. versus* 295 K in this work, cannot account for the difference which is greater than a factor of 2 at 500 Torr. A significant difference between the two studies is the relationship between the propagating laser beams and the direction of flow of the reactant gas. In our work the photolysis and probe lasers counter propagate in a direction that is perpendicular to the direction of gas flow. This means that the gas in the reaction volume is photolyzed only once and replaced by a fresh gas mixture for every laser shot. In contrast, with Wu *et al.*, the photolysis laser is propagating along the direction of flow.

Wu *et al.* state some concerns with their flow configuration noting that "The accumulation of photolytically produced species from multiple laser shots could represent a more serious concern, as the residence time (1.6–1.8 s) is much longer than the laser pulse interval (0.1 s)."

They also note that their pseudo first order plots have large Y intercepts suggesting that a significant loss of BrHg occurs due to side-reactions with other species. They conclude that "Apparently, there are sources of variation or deterministic errors that are not captured by the error bars. The apparent negative curvature of some of the data in these plots further suggests that side reactions are causing significant loss of BrHg."

In our work the values of k' at $[NO_2] = 0$, shown in Table S2,† are reasonable, particularly for the data in N_2 with NO_2 measured by absorption. We should also note that Wu *et al.* measured a smaller range of k', measuring pseudo-first rates of up to $k' = 30\,000\ s^{-1}$. Our results are in better agreement with the calculations of Jiao and Dibble but lie below their high pressure values. Additional work at lower temperatures should shed further light on this.

In their attempt to study reaction (R3) Wu *et al.*[10] found that the $D^2\Pi_{3/2}$ state is quenched rapidly and state that: "To study the reaction of BrHg + O_2 at high $[O_2]$, a different approach, such as cavity ringdown spectroscopy, is needed to quantify and track absolute [BrHg($\tilde{X}$)] without the issue of fluorescence quenching." Our work demonstrates that with a well-designed detection system LIF can detect HgBr in 500 Torr of O_2 with good sensitivity.

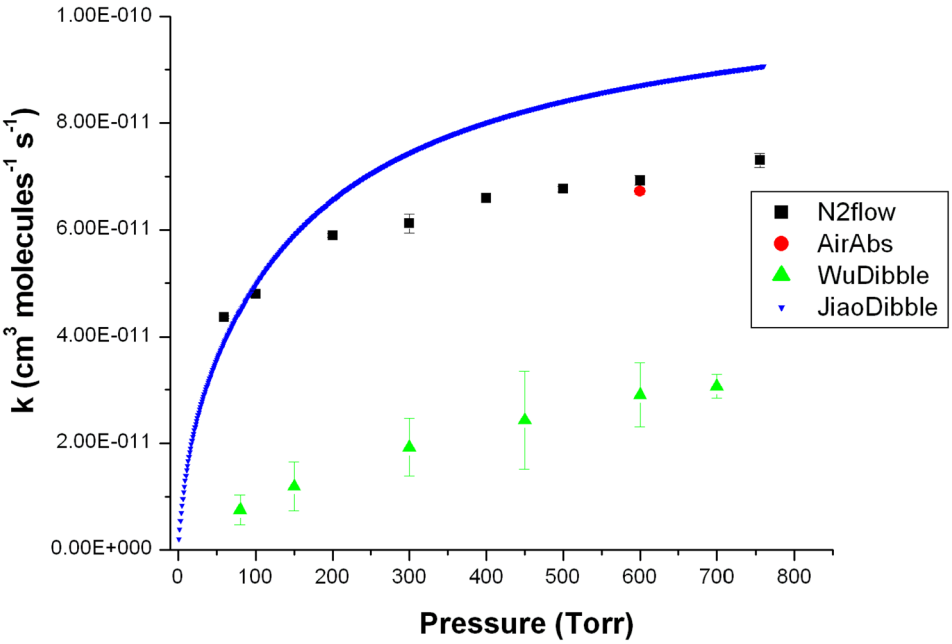

Fig. 10 Comparison of rate coefficients for reaction (R1) based on experimental measurements from this work and that of Wu *et al.*[6] and calculations from Jiao and Dibble.[7]

Possible systematic errors

Measurement of [NO_2]. There have been multiple measurements of NO_2 absorption cross sections in studies of the three body recombination of OH with NO_2. As we noted above we used both broadband and 365 nm absorption to measure [NO_2] in a study of this reaction.[11] A number of subsequent studies have essentially found that 365 nm absorption from a Hg lamp provides an accurate measurement of an NO_2 concentrations. In the most recent study of this reaction Amedro *et al.*[19] remeasured the 365 nm absorption cross-section and also examined the pressure dependence. They measured an absorption cross section of $(5.89 \pm 0.35) \times 10^{-19}$ cm^2 in excellent agreement with the value used in this work, $(5.75 \pm 0.17) \times 10^{-19}$ cm^2. They also present convincing evidence the cross section is independent of pressure.

NO_2 has an absorption cross section of 2×10^{-20} cm^2 at 266 nm which will result in photolysis of ~0.4% of the NO_2 at the photolysis power used in our experiments. At the highest concentration to NO_2 used in our experiments, $\sim 5 \times 10^{15}$ molecules per cm^3 we generate $\sim 2 \times 10^{13}$ molecules per cm^3 of NO and O products. Even if these products reacted with HgBr at a gas kinetic rate they would produce pseudo first order loss rates of ~1000 s^{-1}, a negligible value compared with the experimental loss rate of ~500 000 s^{-1}.

Systematic errors can arise in this type of study if the excess reactant contains a significant amount of impurity that reacts rapidly with HgBr. Another potential systematic error can arise if the photolysis of the $HgBr_2$ precursor produces a reactant that reacts rapidly with HgBr and, as mentioned above, relaxation of vibrationally excited HgBr can be problematic.

NO_2 was purified by freeze–pump cycles at 77 K prior to making reactant mixtures but we were not able to analyze our NO_2 sample for impurities. We do not believe in impurities in our NO_2 sample can account for the difference in the measurements reported in this study and that of Wu *et al.*[6] In particular if we had significant impurities we would not expect the pressure dependence of the reaction to show good three body recombination behavior. This would require the impurity reactant to show an identical pressure dependence which is unlikely.

Any systematic errors associated with the products of $HgBr_2$ photolysis or background levels of Hg(0) would not scale with NO_2 concentration but would rather produce a rapid decay of HgBr in the absence of NO_2 and give a large intercept on k' *versus* NO_2 pseudo first order plots. We see no evidence for any systematic errors resulting from this. Similarly Fig. 8 shows some evidence for vibrational relaxation but this is much too small and much too slow to have any impact on the kinetic studies in the presence of NO_2.

Atmospheric implications

Horowitz *et al.*[8] presented a model for Hg(0) redox chemistry that included rates for HgBr with NO_2 and HO_2 calculated by Jiao and Dibble.[7] The model found that atomic bromine (Br) of marine organobromine origin is the main atmospheric Hg(0) oxidant and that second-stage HgBr oxidation is mainly by the NO_2 and HO_2 radicals. The resulting chemical lifetime of tropospheric Hg(0) against oxidation was 2.7 months, shorter than in previous models. The breakdown of HgBr oxidation in the model is 62% by NO_2, 30% by HO_2 and with less than 10% oxidized *via* reaction with ClO, BrO and OH.

Subsequently reaction (R4) was proposed by Saiz-Lopez *et al.*[20] as an extremely fast reaction essentially proceeding at the hard sphere collision rate.

$$HgBr + O_3 \rightarrow HgBrO + O_2 \quad (R4)$$

Since ozone concentrations are much higher than other potential reactants such as NO_2, reaction (R4) would become the dominant sink for HgBr under most tropospheric conditions. Following the Saiz-Lopez *et al.* hypothesis, Shah *et al.*[21] prosed that steric constraints would lower the rate coefficient of reaction (R4), but they still predicted a fast rate coefficient of 3×10^{-11} cm^3 per molecule per s. They incorporated (R4) with this rate coefficient into the GEOS-Chem global atmospheric chemistry model and found that, using this fast rate, ozone is the dominant sink for HgBr. Gomez Martin *et al.* recently published an experimental study of reaction (R4) and obtained a rate coefficient of $(7.5 \pm 0.6) \times 10^{-11}$ cm^3 per molecule per s. The potential problem in the study of (R4) lies in the fact that the photolysis wavelength that is used to photolyze the HgBr precursor, $HgBr_2$, overlaps the peak of the O_3 absorption spectrum and a significant fraction of the O_3 is photolyzed producing a mixture of O^1D and O^3P. The O^1D is rapidly quenched to O^3P producing an extremely high concentration of O^3P. In the work of Gómez Martin *et al.*[9] they calculated that ~50% of the O_3 present was photolyzed producing equal concentrations of O_3 and O^3P. This study was conducted at low pressures of N_2 with secondary reactions of O atoms dominating the experimental profiles of HgBr. A complex numerical analysis of the experimental temporal profiles was required to extract rate coefficients. We measured the rate coefficient for (R4) in N_2/O_2 mixtures at pressures between 455–750 Torr with O_2 pressures that varied between 270 and 430 Torr. Under these conditions O atoms are rapidly converted to O_3 and do react with HgBr. Hence we obtain good pseudo first order decays of HgBr and obtain a preliminary rate coefficient of $(6.6 \pm 0.7) \times 10^{-11}$ cm^3 per molecule per s in excellent agreement with the value reported by Gómez Martin *et al.*[9] These two experimental studies clearly confirm reaction (R4) is fast and based on the model study of Shah *et al.*[21] confirms that reaction of HgBr with O_3 is the dominant sink of HgBr in the atmosphere.

Conclusions

We have measured the pressure dependent rate coefficient for the reaction of HgBr with NO_2, reaction (R1), in N_2 and He bath gases with a single measurement in air. Our results in N_2 are between a factor of 2 and 3 larger than those reported in recent work by Wu *et al.*[6] and 10 to 15% smaller than the values from the theoretical calculations by Jiao and Dibble.[7]

We monitored Hg(0) production and found no evidence for a reduction channel (R1b). We measured temporal profiles of HgBr in O_2 and found that there is no reaction. Our work demonstrates that with a well-designed detection system LIF can detect HgBr in 500 Torr of O_2 with good sensitivity.

Although we measure fast rate coefficients for reaction (R1) recent work on the reaction of O_3 with HgBr suggests this will be the dominant oxidation process for HgBr in the atmosphere.

Data availability

The most critical data, the pressure and bath gas dependence of the rate coefficients for reaction (R1) are listed in the ESI,† will be uploaded to an accessible database upon the manuscript's publication.

Author contributions

Conceptualization: AJH, DB; formal analysis: AJH, DB; funding acquisition: AJH; detection design: DD; writing: AJH, DB.

Conflicts of interest

There are no conflicts to declare.

Acknowledgements

This work was supported the National Science Foundation under award number 2003976. We thank Elliot Atlas for helpful discussions and logistical support and Nicholas Forcone for support in the development of the data acquisition software.

References

1 United Nations Environment Program, *Global Mercury Assessment 2018*, United Nations, 2019, **https://wedocs.unep.org/20.500.11822/27579**, accessed April 2025.
2 C. J. Lin and S. O. Pehkonen, The chemistry of atmospheric mercury: a review, *Atmos. Environ.*, 1999, **33**, 2067.
3 W. H. Schroeder and J. Munthe, Atmospheric mercury—an overview, *Atmos. Environ.*, 1998, **32**, 809–822.
4 F. Slemr, E. G. Brunke, R. Ebinghaus and J. Kuss, Worldwide trend of atmospheric mercury since 1995, *Atmos. Chem. Phys.*, 2011, **11**, 4779–4787.
5 D. L. Donohoue, D. Bauer, B. Cossairt and A. J. Hynes, Temperature and pressure dependent rate coefficients for the reaction of Hg with Br and the reaction of Br with Br: a pulsed laser photolysis pulsed laser induced fluorescence study, *J. Phys. Chem. A*, 2006, **110**, 6623–6632.
6 R. Wu, C. Wang and T. S. Dibble, First experimental kinetic study of the atmospherically important reaction of BrHg + NO_2, *Chem. Phys. Lett.*, 2020, **759**, 137928.
7 Y. Jiao and T. S. Dibble, First kinetic study of the atmospherically important reactions BrHg + NO_2 and BrHg + HOO, *Phys. Chem. Chem. Phys.*, 2017, **19**, 1826–1838.
8 H. M. Horowitz, D. J. Jacob, Y. Zhang, T. S. Dibble, F. Slemr, H. M. Amos, J. A. Schmidt, E. S. Corbitt, E. A. Marais and E. M. Sunderland, A new mechanism for atmospheric mercury redox chemistry: implications for the global mercury budget, *Atmos. Chem. Phys.*, 2017, **17**, 6353–6371.
9 J. C. Gómez Martín, T. R. Lewis, K. M. Douglas, M. A. Blitz, A. Saiz-Lopez and J. M. C. Plane, The reaction between HgBr and O3: kinetic study and atmospheric implications, *Phys. Chem. Chem. Phys.*, 2022, **24**, 12419–12432.
10 R. Wu, P. J. Castro, K. C. Gaito, T. S. Dibble and C. Wang, Combined experimental and computational kinetics studies for the atmospherically important BrHg radical reacting with NO and O_2, *J. Phys. Chem. A*, 2022, **126**, 3914–3925.

11 L. D'Ottone, P. Campuzano-Jost, D. Bauer and A. J. Hynes, A pulsed laser photolysis-pulsed laser induced fluorescence study of the kinetics of the gas-phase reaction of OH with NO_2, *J. Phys. Chem. A*, 2001, **105**, 10538–10543.
12 D. L. Donohoue, PhD thesis, University of Miami, 2008.
13 J. H. Parks, Laser action on the $B^2\Sigma^+_{1/2} \rightarrow X^2\Sigma^+_{1/2}$ band of HgBr at 5018 Å, *Appl. Phys. Lett.*, 1977, **31**, 297.
14 P. H. Wine, N. M. Kreutter and A. R. Ravishankara, Flash photolysis-resonance fluorescence kinetics study of the reaction OH + NO_2 + M → HNO_3 + M, *J. Phys. Chem.*, 1979, **83**, 3191–3195.
15 M. S. Landis, R. K. Stevens, F. Schaedlich and E. M. Prestbo, Development and characterization of an annular denuder methodology for the measurement of divalent inorganic reactive gaseous mercury in ambient air, *Environ. Sci. Technol.*, 2002, **36**, 3000–3009.
16 J. Maya, Ultraviolet absorption cross sections of HgI_2, $HgBr_2$, and tin(II) halide vapors, *J. Chem. Phys.*, 1977, **67**, 4976–4980.
17 M. B. Williams, P. Campuzano-Jost, A. J. Pounds and A. J. Hynes, Experimental and theoretical studies of the reaction of the OH radical with alkyl sulfides: 2 kinetics and mechanism of the OH initiated oxidation of methylethyl and diethyl sulfides; observations of a two channel oxidation mechanism, *Phys. Chem. Chem. Phys.*, 2007, **9**, 4370–4382.
18 M. B. Williams, P. Campuzano-Jost, B. M. Cossairt, A. J. Hynes and A. J. Pounds, Experimental and theoretical studies of the reaction of the OH radical with alkyl sulfides: 1 direct observations of the formation of the OHDMS adduct – pressure dependence of the forward rate of addition and development of a predictive expression at low temperature, *J. Phys. Chem. A*, 2007, **111**, 89–104.
19 D. Amedro, A. J. C. Bunkan, M. Berasategui and J. N. Crowley, Kinetics of the OH + NO_2 reaction: rate coefficients (217–333 K, 16–1200 mbar) and fall-off parameters for N_2 and O_2 bath gases, *Atmos. Chem. Phys.*, 2019, **19**, 10643–10657.
20 A. Saiz-Lopez, O. Travnikov, J. E. Sonke, C. P. Thackray, D. J. Jacob, J. Carmona-García, A. Frances-Monerris, D. Roca-Sanjuan, A. U. Acuna, J. Z. Davalos, C. A. Cuevas, M. Jiskra, F. Wang, J. Bieser, J. M. C. Plane and J. S. Francisco, Photochemistry of oxidized Hg(I) and Hg(II) species suggests missing mercury oxidation in the troposphere, *Proc. Natl. Acad. Sci. U.S.A.*, 2020, **117**, 30949–30956.
21 V. Shah, D. J. Jacob, C. P. Thackray, X. Wang, E. M. Sunderland, T. S. Dibble, A. Saiz-Lopez, I. Cernusak, V. Kello, P. J. Castro, R. Wu and C. Wang, Improved mechanistic model of the atmospheric redox chemistry of mercury, *Environ. Sci. Technol.*, 2021, **55**, 14445–14456.